# Supplementary Material for Efficient Rare Event Sampling with Unsupervised Normalising Flows

**Solomon Asghar**[1,2,3], **Qing-Xiang Pei**[2], **Giorgio Volpe**[1*], **and Ran Ni**[3*]

[1]Department of Chemistry, University College London, 20 Gordon Street, WC1H 0AJ London, United Kingdom
[2]A*STAR, Institute of High Performance Computing, Singapore, 138632, Singapore
[3]School of Chemistry, Chemical Engineering and Biotechnology, Nanyang Technological University, Singapore, 639798, Singapore
[*]g.volpe@ucl.ac.uk and r.ni@ntu.edu.sg

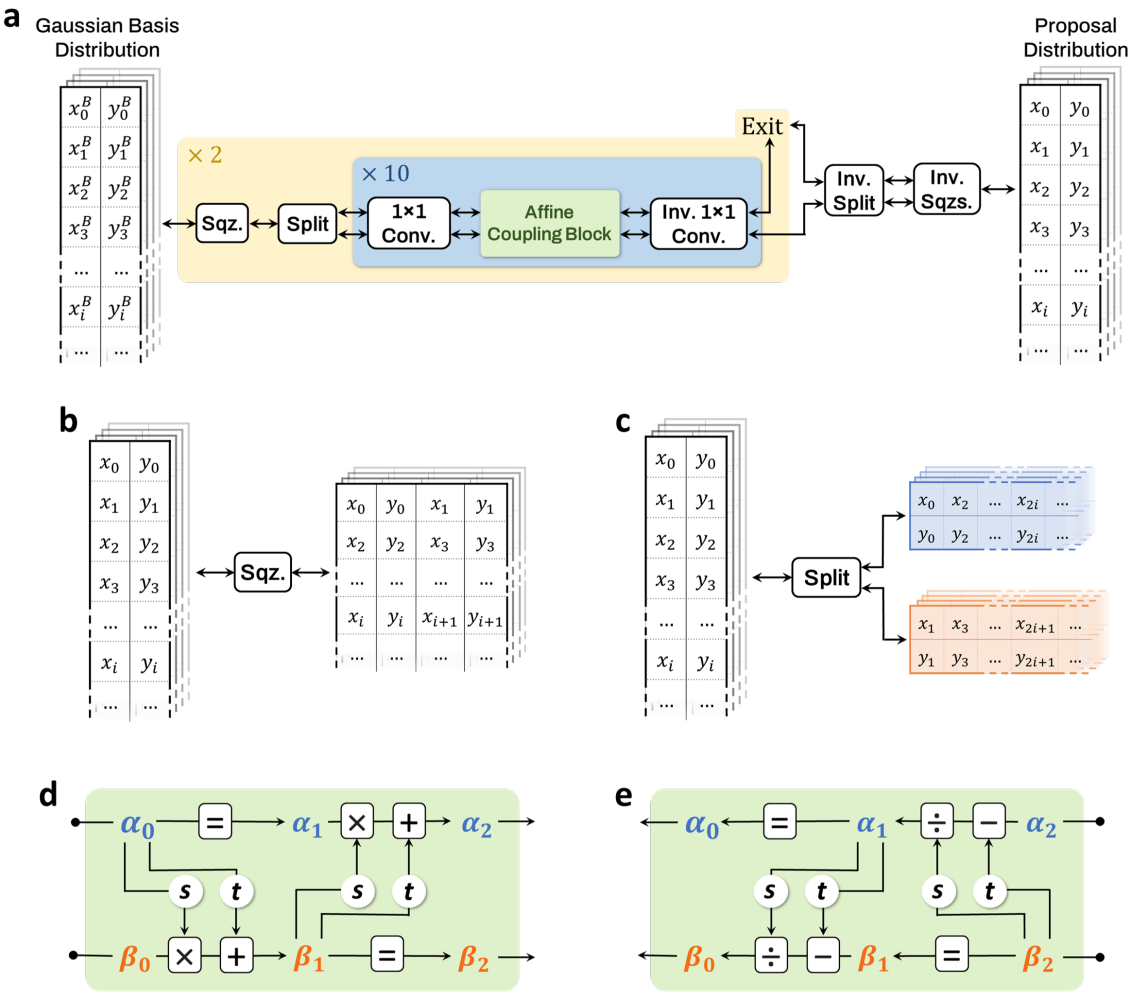


**Figure S1. FlowRES normalising flow network architecture for passive systems.** (**a**) FlowRES network for passive systems. Input Gaussian basis matrices are passed into the first of 2 *scales* (Methods), which begin by reshaping the input with a squeeze operation (see **b**) followed by dividing it into two channels with an alternating split (see **c**). The two channels are passed to 10 consecutive *complete flow steps*, each composed of an *affine coupling block* (see **d** and **e**) preceded by a $1 \times 1$ convolution and followed by the inverse of this convolution. After the complete flow steps, one of the two channels is factored out while the other channel passes on to the next scale. After both scales, all the squeeze operations and splits are inverted, yielding a distribution of proposed paths. (**b**) In a squeeze operation, the matrices in a channel all change shape, doubling in width but halving in height. A squeeze is equivalent to an alternating split (see **c**) followed by the two resulting channels being horizontally concatenated. (**c**) In an alternating split, a single channel is split into two. Even indices form one channel (blue) and odd indices form another (red). (**d**) An affine coupling block used when generating path proposals. The channel $\alpha_0$ is passed into two WaveNet networks (Methods), the outputs of which parameterize a bijective transformation $\beta_1 = \beta_0 \odot \exp[s(\alpha_0)] + t(\alpha_0)$ of the second channel $\beta_0$. This new $\beta_1$ is then passed into other WaveNets, whose outputs are used to parameterize $\alpha_2 = \alpha_1 \odot \exp[s(\beta_1)] + t(\beta_1)$. (**e**) An inverted affine coupling block (used when training).

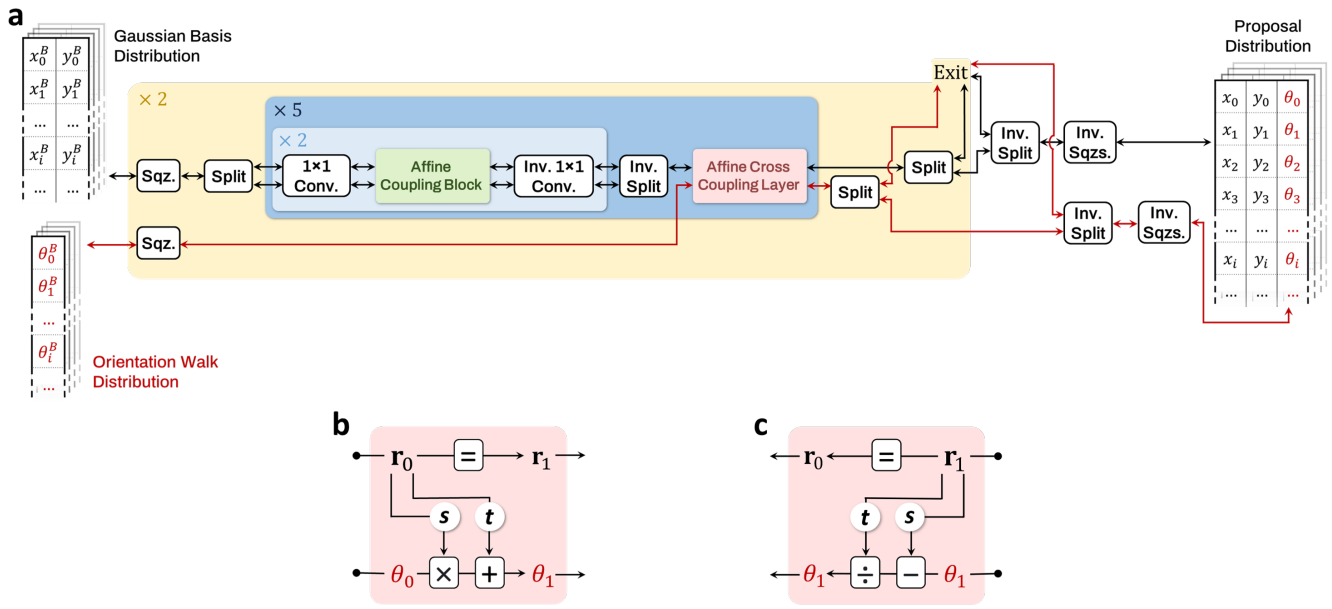


**Figure S2. FlowRES normalising flow network architecture for active systems.** (**a**) As with the passive case in Fig. S1a, input Gaussian basis matrices are passed into the first of 2 *scales* (Methods); these matrices will be transformed to form the position component of the final proposed paths. Alongside these, the orientations of a random walk are also passed to the scales. Both of these inputs are reshaped with squeeze operations (Fig. S1b). The squeezed Gaussian basis matrices are divided into two channels with an alternating split (Fig. S1c), and these two position channels (black lines) are then passed to 5 *complete flow steps*: each step is first composed of two affine coupling blocks sandwiched between $1 \times 1$ convolutions and inverse $1 \times 1$ convolutions (Fig. S1d-e); after these two affine coupling blocks, the two position channels are recombined and fed alongside the orientation walk into an angle cross-coupling layer (see **b-c**). A position channel and orientation channel are the output of this coupling layer. Each of these then undergo alternating splits (Fig. S1c), with one channel from each being factored out and the other moving onward to the next scale. After both scales, all the squeeze operations and splits are inverted. Combining the position and orientation channels yields a distribution of proposed paths. (**b**) An affine cross-coupling layer used when generating path proposals. The orientation channel $\theta$ is passed into two WaveNet networks (Methods), the outputs of which parameterize a bijective transformation that updates the position channel: $\mathbf{r}_1 = \mathbf{r}_0 \odot \exp[s(\theta_0)] + t(\theta_0)$. Note that the orientation channel itself remains unchanged by this layer. (**c**) An inverted affine cross-coupling layer, used for training.

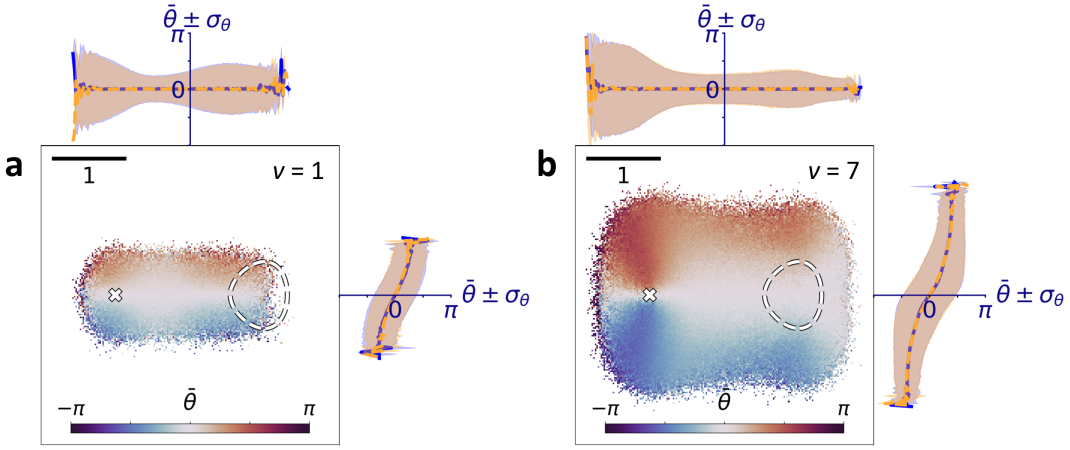


**Figure S3. Orientations of active Brownian particles for barrier crossing in a double-well potential.** The color maps show FlowRES-generated average orientations $\bar{\theta}$ at different points on a double-well potential (Fig. 2a, barrier height of $15\,k_{\mathrm{B}}T_{\mathrm{eff}}$ as in Fig. 3a-b) for target-reaching active Brownian particles with (**a**) $v = 1$ and (**b**) $v = 7$. These are flanked by lines showing the average orientations at different $x$ (above) and $y$ (right) values (standard deviations given as shaded regions) generated by FlowRES (blue lines and shaded blue regions) and by direct integration (dashed yellow lines and shaded yellow regions) of Langevin equations (Eqs. 1 and 2). Note the strong correspondence between both results. Starting point (white cross) and target region (dashed line) are shown for reference. Unitary scale bar: upper left. Simulation parameters as in Fig. 3a-b.

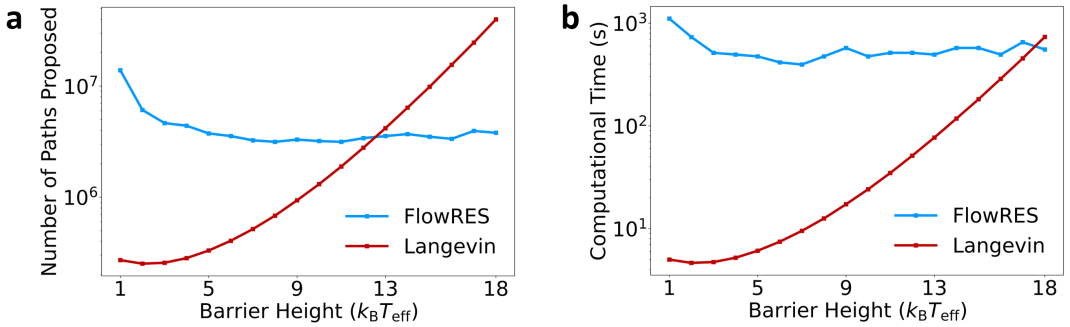


**Figure S4. Computational efficiency for barrier crossing of active Brownian particles in a double-well potential.** (**a**) Total number of active particles' paths ($v = 1$) proposed to yield 10,000 target-reaching paths with null JSD deviation (Methods) and (**b**) corresponding computational time with FlowRES (blue line) and direct integration (red line) as a function of barrier height of the double-well potential in Fig. 2a. The computational cost of direct integration of Langevin equations increases exponentially with barrier height, while FlowRES maintains near constant computational cost. Simulation parameters as in Fig. 3a.

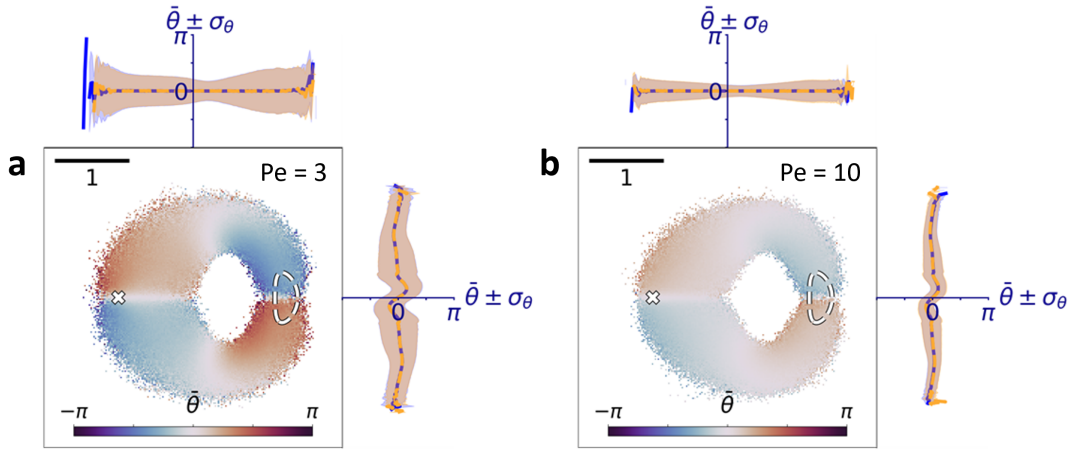


**Figure S5. Orientations of active Brownian particles for circumventing an insurmountable wall on a double-well potential.** The color maps show FlowRES-generated values for average orientations $\overline{\theta}$ at different points on a double-well potential with an insurmountable wall separating them (Fig 3c, Methods) for target-reaching active Brownian particles with (**a**) Pe = 3 and (**b**) Pe = 10. These are flanked by lines showing the average orientations at different $x$ (above) and $y$ (right) values (standard deviations given as shaded regions) generated by FlowRES (blue lines and shaded blue regions) and by direct integration (dashed yellow lines and shaded yellow regions) of Langevin equations (Eqs. 1 and 2). Note the strong correspondence between both results. Starting point (white cross) and target region (dashed line) are shown for reference. Unitary scale bar: upper left. Simulation parameters as in Fig. 3d-e.

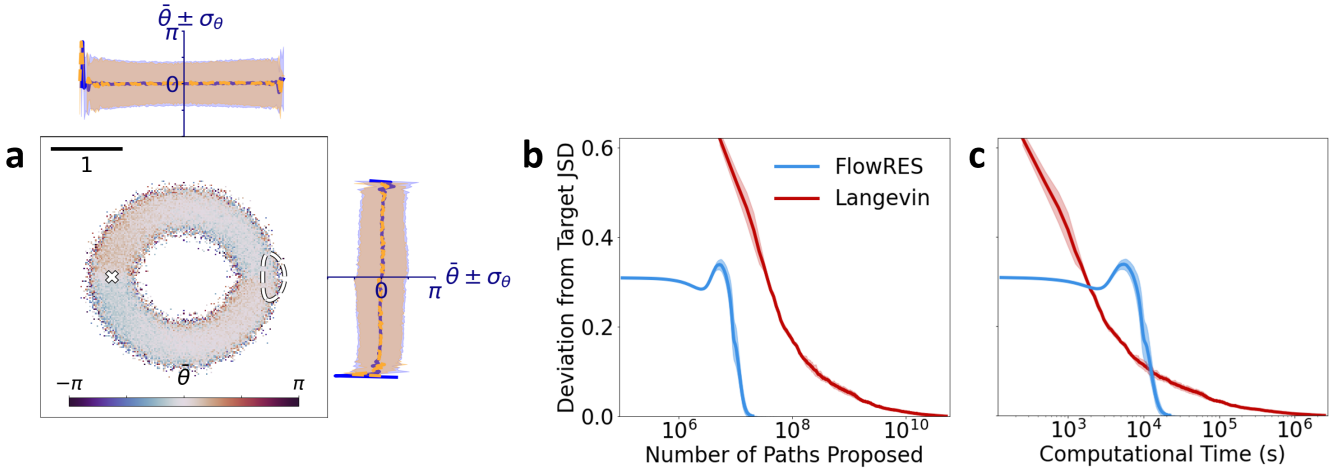


**Figure S6. Enhanced sampling of active Brownian particles exploring an asymmetric dual-channel double-well potential.** (**a**) The color map shows FlowRES-generated values for the average orientations $\overline{\theta}$ at different points on a dual-channel double-well potential (Fig. 4a, Methods) for target-reaching active Brownian particles. This is flanked by lines showing the average orientations at different $x$ (above) and $y$ (right) values (standard deviations given as shaded regions) generated by FlowRES (blue lines and shaded blue regions) and by direct integration (dashed yellow lines and shaded yellow regions) of Langevin equations (Eqs. 1 and 2). Note the strong correspondence between both results. Starting point (white cross) and target region (dashed line) are shown for reference. Unitary scale bar: upper left. Simulation parameters as in Fig. 4. (**b-c**) Average deviations of the Jensen Shannon distance (JSD) between validation ensemble and ensembles of target-reaching paths generated with FlowRES (blue lines) and direct integration (red lines) from the target JSD (Methods) as a function of (**b**) the number of paths proposed and (**c**) the computational time. Shaded areas represent standard deviations around the average from five independent simulations.